Ionothermal synthesis of bismuth sulfide nanostructures and their electrochemical hydrogen storage behavior

Qingtao Wang,[ac] Xiaobo Wang,[a] Wenjing Lou*[a] and Jingcheng Hao*[ab]

Received (in Gainesville, FL, USA) 8th January 2010, Accepted 26th March 2010
DOI: 10.1039/c0nj00009d

Bismuth sulfide (Bi_2S_3) nanoflowers and nanorods were synthesized by thermal decomposition of single source precursor, bismuth di-*n*-octyl-dithiophosphate ($Bi[S_2P(OC_8H_{17})_2]_3$), in an ionic liquid (IL) solvent. Both of these products belong to the orthorhombic phase by the analysis of the X-ray powder diffraction spectra. The morphology evolution of Bi_2S_3 from nanoflowers to nanorods was investigated based on transmission electron microscopy observations. The electrochemical hydrogen storage behavior of these Bi_2S_3 nanostructures was studied in detail. It was found that the morphology and structure played an important role on the hydrogen storage capacity of such nanomaterials. The Bi_2S_3 nanoflower structures have a discharging capacity of 100 mAh g^{-1} at room temperature, which makes it a potential candidate for applications in hydrogen storage, high-energy batteries, and catalytic fields.

Introduction

Semiconducting metal chalcogenides such as A_2B_3 (A = Bi, Sb, As; B = S, Se, Te) compounds are widely applied in hologram storage technology, optical memory devices, and IR spectroscopy.[1–3] Among these semiconductors, bismuth sulfide (Bi_2S_3), a direct bandgap semiconductor with E_g of 1.3 eV,[4] has found applications in photoelectric conversion,[5] photosensors,[6] and electrochemical hydrogen storage.[7] Recently, considerable efforts have been focused on the controlled synthesis of one-dimensional (1D) Bi_2S_3 nanostructures as well as their ordered arrays or complex assemblies. Simple 1D Bi_2S_3 nanostructures such as nanorods, nanowires, and nanobelts can be produced by micelle-template method,[8] solvothermal or hydrothermal process,[9] and solventless thermolysis.[10] Bi_2S_3 nanowire architectures have been fabricated by a microwave-hydrothermal method[11] and by using a colloidal solution method[12] or ionic liquid-assisted reaction system.[13] The controlled synthesis of 1D nanostructures and guiding them to ordered arrays or complex functional architectures would offer great opportunities to explore their novel properties and to fabricate useful nanodevices.[14]

Recently, ionic liquids (ILs) have been actively investigated as alternative solvent media in synthesis, catalysis, separation, and electrochemistry.[15] These solvent systems offer a novel chemical environment that can uniquely influence the course of chemical reactions compared to those traditional solvents. As new reaction media, ILs have many advantages in the inorganic nanomaterial synthetic field. Some of them possess low interface tension, which results in high nucleation rates, so very small particles can be generated.[16] Extended hydrogen bond systems can be formed in the liquid state[17] and this special quality is useful for spontaneous, well-defined, and extended ordering of nanoscale structures.[16] Suitable ILs as reaction media were attempted to synthesize novel nanostructured particles such as hollow TiO_2 microspheres,[18] Au nanoparticles,[19] mesoporous silica nanoparticles,[20] CoPt nanorods,[21] and Rh nanoparticles.[22]

Herein we reported the preparation of crystalline Bi_2S_3 nanoflowers and nanorods, which were synthesized by solvothermal treatment of bismuth di-*n*-octyl-dithiophosphate ($Bi[S_2P(OC_8H_{17})_2]_3$) in an ionic liquid ($C_{16}MIMBF_4$) solvent. The size and aspect ratio of the product strongly depended on the reaction time. So the morphology of the product can be tailored by controlling the reaction time. The electrochemical hydrogen storage behaviors of these Bi_2S_3 nanostructures were investigated. It was found that the morphology of such nanomaterials is related to their electrochemical hydrogen storage behaviors.

Results and discussion

Morphology evolution of Bi_2S_3 nanocrystals with increasing reaction time

The Bi_2S_3 nanostructures at various stages of the growth process were characterized using transmission electron microscopy (TEM) and field emission scanning electron microscopy (FE-SEM), as shown in Fig. 1 and 2. Before reaction, the mixed solution was light yellow-green and transparent. The solution became dark gray quickly after heat treatment for 3 s. Small irregularly shaped particles with an average diameter of 80 nm and several aggregations with an average diameter of 250 nm can be observed in Fig. 1a. With the reaction time increasing to 5 s, the morphology of the products changed greatly. Large numbers of flower-like nanostructures with an average diameter of 250 nm came into being (Fig. 1b). Most of the irregular-shaped particles disappeared. When the reaction time increased to 5 min, the diameter of these flower-like

[a] *State Key Laboratory of Solid Lubrication, Lanzhou Institute of Chemical Physics, Chinese Academy of Sciences, Lanzhou, China. E-mail: wjlou@licp.cas.cn, jhao@sdu.edu.cn; Fax: +86 531 88366074; Tel: +86 531 88366074*
[b] *Key Laboratory for Colloid and Interface Chemistry of Education Ministry, Shandong University, Jinan, China*
[c] *Graduate School of Chinese Academy of Sciences, Beijing, China*

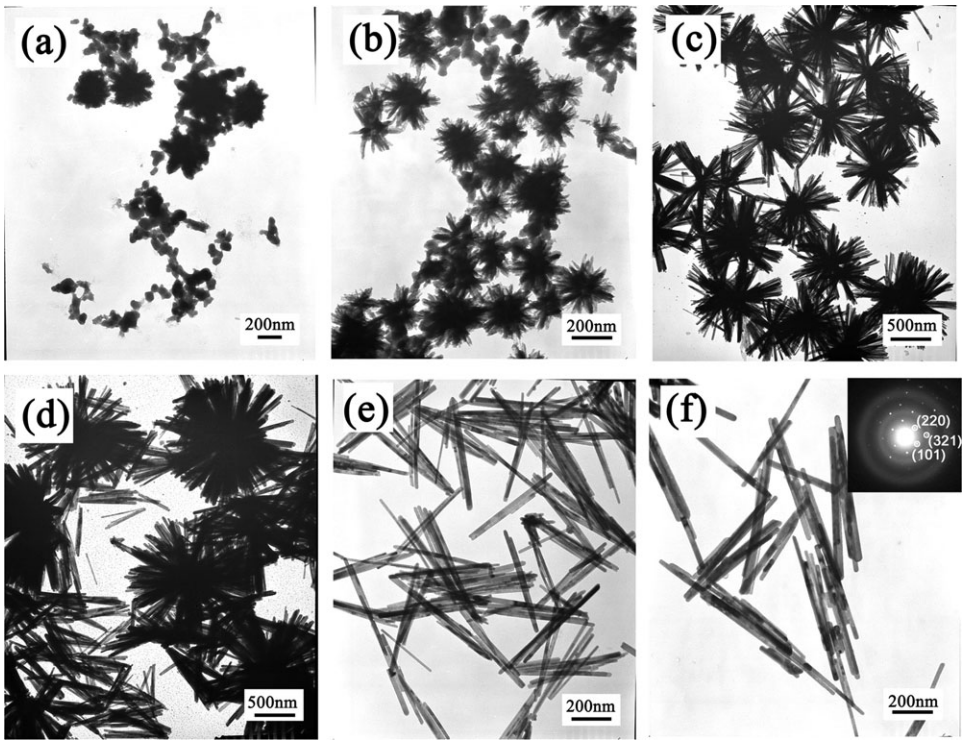

Fig. 1 TEM images of Bi_2S_3 prepared at different reaction times: (a) 3 s, (b) 5 s, (c) 5 min, (d) 30 min, (e) 1 h, and (f) 5 h with inserting the SAED pattern of the single Bi_2S_3 nanorods.

nanostructures increased to 900 nm and these nanostructures consisted of many nanorods with uniform size and length (Fig. 1c and 2a). Compared with Fig. 1b, the density of leaves decreased with the increase in their length. An energy-dispersive spectroscopy (EDS) spectrum (Fig. 2b) was used to illuminate the composition of the flower-like nanostructures. The atom ratio of Bi to S was 40.61 : 59.39, which matches well with the stoichiometric ratio, 2 : 3, of the compound of Bi_2S_3. When the reaction time prolonged to 30 min, both the length and the density of the leaves in these flower-like nanostructures increased (Fig. 1d). The diameter of the flower-like Bi_2S_3 nanostructures was about 1.1 μm. Some disheveled nanorods dispersed around them.

After 1 h, only nanorods with an average length of 600 nm and diameter of 30 nm were obtained and flower-like nanostructures disappeared (Fig. 1e). After reacting for 5 h, the average length of nanorods increased to 800 nm with the average diameter slightly increasing to 33 nm (Fig. 1f and 2c). The combined analysis of the selected area electron diffraction (SAED) pattern inserted in Fig. 1f and EDS spectrum in Fig. 2d indicate that these nanorods were single-crystalline Bi_2S_3 phase. For the reaction time longer than 5 h, the length of these nanorods still increased slowly but no changes occurred to the morphology and diameter.

To further investigate the crystalline phase of these products obtained at different reaction times, these powders were examined by X-ray diffraction (XRD), as shown in Fig. 3. The standard line pattern of orthorhombic Bi_2S_3 was also appended at the bottom. Although several weak and broad peaks appeared for the product of 5 s (Fig. 3A), the positions of these peaks could be separately indexed to (130), (211), (221), (431), (501), and (351) planes of bismuthinite. This result indicates that it was facile to obtain crystalline Bi_2S_3 under this reaction condition within a very short reaction time of 5 s. When the reaction time was longer than 5 min, the diffraction peaks in the corresponding patterns became narrower and stronger (Fig. 3B–D). The positions of all the peaks of the products obtained at different reaction times matched with the standard pattern of the orthorhombic Bi_2S_3 phase (JCPDS Card no. 17-0320) very well. These peaks became stronger with the increase of reaction time, indicating that the crystals of Bi_2S_3 gradually grew well.

Possible crystalline growth mechanism of Bi_2S_3 nanostructures

To understand the rupture of Bi_2S_3 nanoflowers into nanorods, the microstructures of the sample prepared at 30 min which consisted of nanoflowers and nanorods, were investigated by high-resolution TEM (HRTEM) in Fig. 4. The fragments of nanoflowers appeared to be sector shaped and bowknot shaped structures in Fig. 4a. The vestiges of rupture, marked with the white line in Fig. 4b and c, can be clearly distinguished at the root of the sector shaped fragment. Fig. 4c indicates that the rupture part was acuminate, which was highly crystallized and free from dislocation and stacking faults. Similarly, the lattice image of the junction of the bowknot-like fragment also indicated its high crystallinity (Fig. 4d). Based on the above analysis, it is concluded that not only the leaves but also the flower hearts were all crystalline in Bi_2S_3 nanoflowers.

On the basis of experimental results and the discussion, a possible mechanism for the formation of two Bi_2S_3 nanostructures is proposed and displayed in Scheme 1. At the

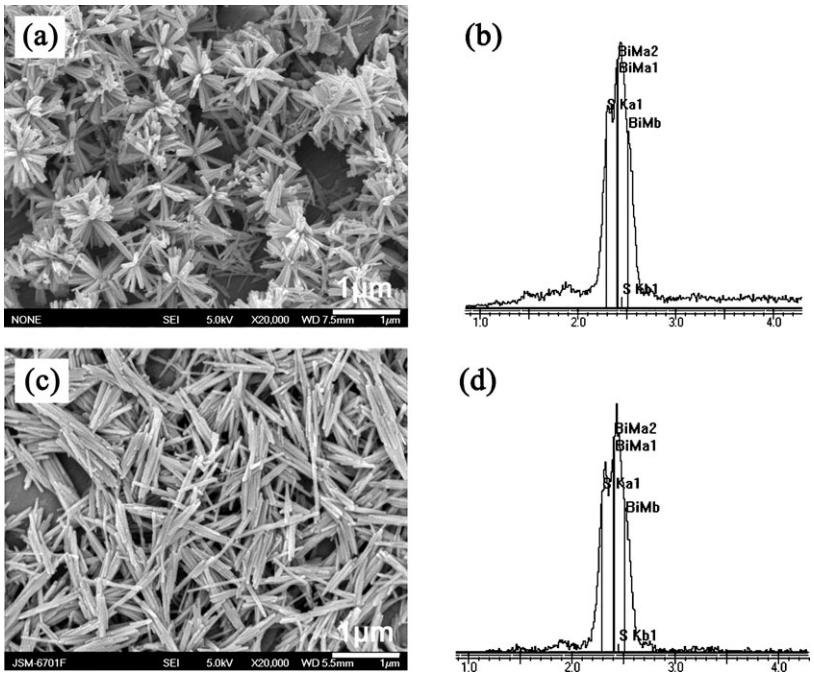

Fig. 2 FE-SEM images and the corresponding EDS spectra of Bi_2S_3 nanoflowers and nanorods prepared for 5 min (a and b) and 5 h (c and d).

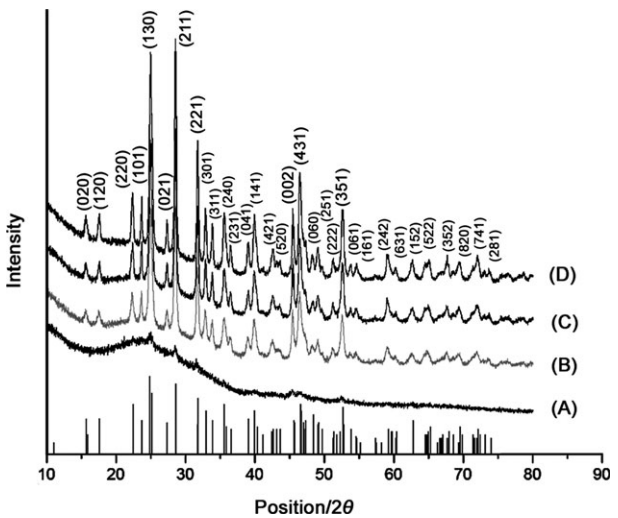

Fig. 3 Time-dependent XRD patterns of Bi_2S_3 prepared at different reaction times: (A) 5 s, (B) 5 min, (C) 1 h, and (D) 5 h. The bottom line pattern is the standard pattern of Bi_2S_3.

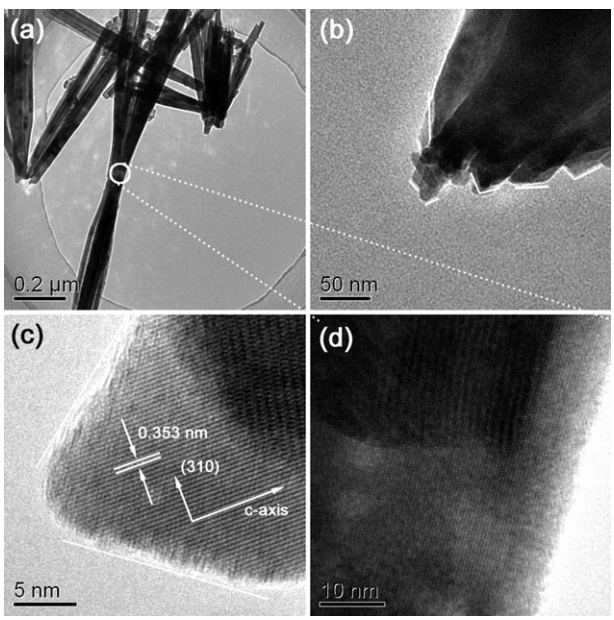

Fig. 4 TEM images of Bi_2S_3 prepared at 30 min. (a) Sector shaped and bowknot shaped fragment, (b) the root of the sector shaped fragment, (c) a high-resolution image of the ruptured part and (d) the junction of the bowknot-like fragment.

beginning, the reaction was so fast that lots of amorphous and poorly crystalline nanoparticles formed along with the aggregations, which can be supported by the TEM image (Fig. 1a) and XRD pattern (Fig. 3A). The nucleation of crystalline Bi_2S_3 randomly adsorbed onto the surfaces of these aggregations rapidly. Then, the surface Bi_2S_3 crystal grew into 1D structures depended on its intrinsic nature. As reported previously,[4,23] Bi_2S_3 is a highly anisotropic semiconductor with layered structure parallel to the growth direction (*c*-axis). With the growth of surface nanorods, the amorphous core dissolved into the solution and served as the source for the growth of nanorods,[24] which is a typical Ostwald ripening process. At the same time, the cores of nanoflowers crystallized. Because of the strain or stress caused by the mismatch of crystal lattices or the over high ratio of length to diameter of the leaves, the flower hearts could not support the leaves of nanoflowers any more. So the rupture occurred at this time. With the further ageing, the independent nanorods formed eventually.

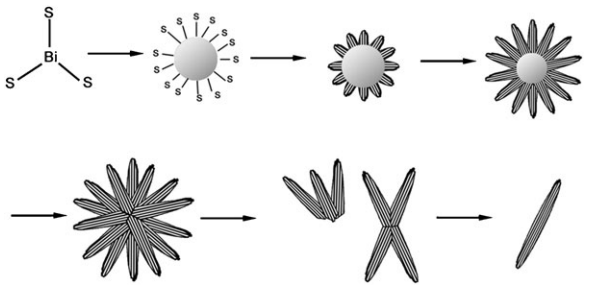

Scheme 1 Proposed growth mechanism for the formation of Bi_2S_3 nanoflowers and nanorods.

Electrochemical hydrogen storage behaviors of Bi_2S_3 nanoflowers and nanorods

The electrochemical hydrogen storage behaviors of the Bi_2S_3 nanocrystals were measured at a constant current density of 50 mA g^{-1}. Their charge-discharge voltage curves are shown in Fig. 5. Fig. 5a shows the charging curve of Bi_2S_3 nanoflowers prepared at 5 min. Two plateaus around −0.68 V (*vs* Hg/HgO) and −0.8 V indicate the presence of two different hydrogen adsorption sites for the Bi_2S_3 nanoflower structures.[7] It was assumed that the hydrogen was first adsorbed onto the interstitial pores among Bi_2S_3 rodlike petals in the nanoflower structures and then entered into the interlayers of Bi_2S_3 crystals. The plateau of the discharging potential appeared at −0.5 V *versus* Hg/HgO and a discharging capacity of 100 mAh g^{-1} was obtained. This result implies that the Bi_2S_3 nanoflowers can be used as a material for electrochemical hydrogen storage. When the electrode material was replaced by the Bi_2S_3 nanorods prepared at 5 h (Fig. 5b), the discharging capacity was measured to be 83 mAh g^{-1}. This result was lower than that of Bi_2S_3 nanoflowers, which may be relate to the less interstitial pores in nanorods than in nanoflowers.[7] Overall, the capacity of electrochemical hydrogen storage of the final products was sensitive to the morphology and microstructures of Bi_2S_3 crystals.

Cyclic voltammograms (CVs) were carried out to further investigate the electrochemical hydrogen adsorption–desorption behavior of Bi_2S_3 nanocrystals. In Fig. 6a, an obvious cathodic adsorption/reduction peak of hydrogen (H_{ads}) appeared at *ca.* −0.78 V *versus* Hg/HgO. During the following anodic polarization, two current peaks appeared at *ca.* −0.53 V and −0.40 V, which are attributed to the hydrogen desorption (H_{des}) and hydrogen oxidation (H_{oxi}),[25] respectively. The phenomenon of the hydrogen desorption peak prior to the hydrogen oxidation peak means the possible existence of the strong chemisorption of hydrogen, similar to the observation and discussion for CV curves of BN nanotubes.[26] For the CVs of Bi_2S_3 nanorods (Fig. 6b), a broad cathodic peak appeared at *ca.* −0.88 V, lower than that of the nanoflowers electrode, and two weak anodic peaks appeared at *ca.* −0.50 V and −0.39 V, higher than those for the nanoflower electrode. This result suggested that both adsorption/reduction and desorption/oxidation of hydrogen were more difficult on the Bi_2S_3 nanorods. Furthermore, the desorption/oxidation peaks of Bi_2S_3 nanoflowers were stronger than those of Bi_2S_3 nanorods, suggesting that the flower-like structures of Bi_2S_3 nanocrystals were better than the rodlike structures in hydrogen storage behavior.

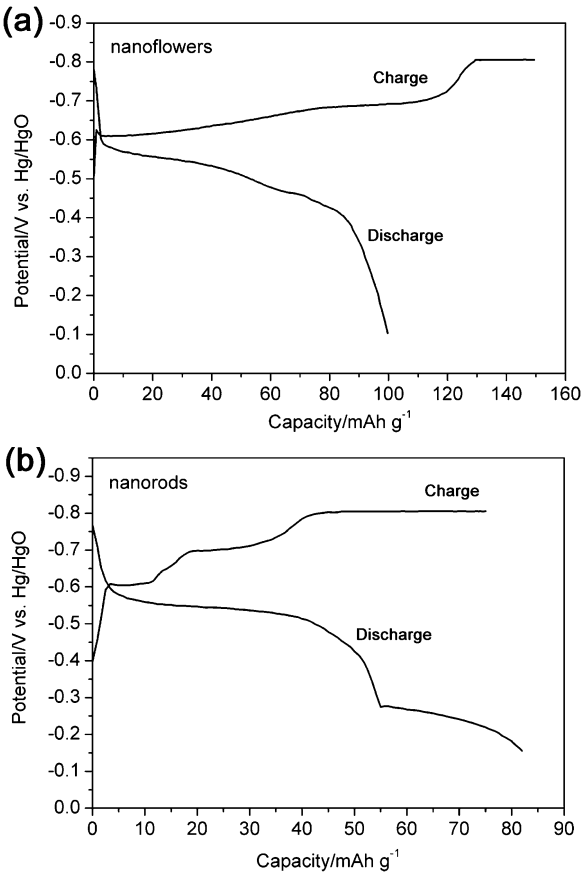

Fig. 5 Charge-discharge curves of Bi_2S_3 nanocrystals: (a) nanoflowers prepared at 5 min and (b) nanorods prepared at 5 h. Current density: 50 mA g^{-1}.

Conclusions

In the present paper, Bi_2S_3 nanostructures were synthesized by thermal treatment of a single-source precursor in ILs media. The morphology of the nanocrystals changed from nanoflowers to nanorods gradually with the increasing of reaction time. Charge-discharge curves and cyclic voltammograms of the obtained Bi_2S_3 nanostructures were measured to investigate their electrochemical hydrogen storage behaviors. The capacity of electrochemical hydrogen storage is sensitive to the morphology and microstructure of Bi_2S_3 nanocrystals. The flower-like Bi_2S_3 nanostructures have a discharging capacity of 100 mAh g^{-1} at room temperature, indicating their potential applications in hydrogen storage, high-energy batteries, and catalytic fields. This method is expected to be applicable to the preparation of nanostructures of other metal sulfide compounds.

Experimental

Materials and characterization

All reactants and solvents used in the experiment were analytical grade. Ammonium *O*,*O*′-di-*n*-octyl-dithiophosphate was obtained from Alfa Aesar and other reagents were purchased from Sinopharm Chemical Reagent Co. Ltd. Water was triply distilled and 1-methylimidazole was distilled before used. Other reagents were used without further purification.

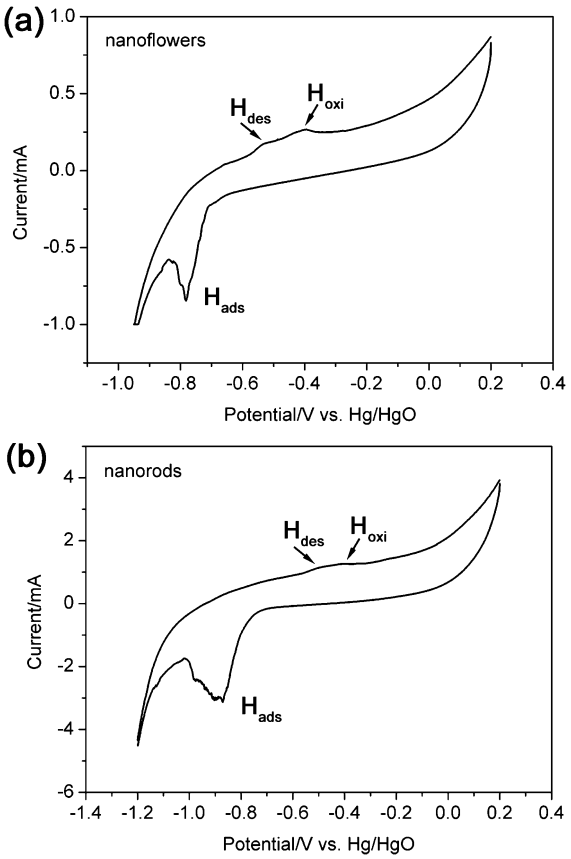

Fig. 6 Cyclic voltammograms of Bi_2S_3 nanocrystal electrodes: (a) nanoflowers prepared at 5 min and (b) nanorods prepared at 5 h.

Transmission electron microscopy (TEM) and selected area electron diffraction (SAED) were performed with an H-600 Electron Microscopy (HITACHI, Japan) operating at 100 kV accelerating voltage. Scanning electron microscopy images were obtained on a JSM-6701F field emission scanning electron microscopy (FE-SEM) operated at 5.0 kV and energy-dispersive spectroscopy (EDS) were performed on a JSM-5600LV scanning electron microscopy operated at 20.0 kV. Powder X-ray diffraction (XRD) patterns were obtained on a RigaKu D/max-RB diffractometer with Cu-Kα radiation (λ = 1.54056 Å) under 40 kV and 30 mA by scanning between 10° and 80° (2θ). High-resolution TEM were performed on a JEM-2010 transmission electron microscopy operated at 200 kV.

Synthesis of bismuth di-*n*-octyl-dithiophosphate ($Bi[S_2P(OC_8H_{17})_2]_3$)

$Bi[S_2P(OC_8H_{17})_2]_3$ was prepared by a reaction of bismuth (III) nitrate with ammonium *O*,*O*′-di-*n*-octyl-dithiophosphate in the mixed solution of water and ethanol at room temperature overnight according to the reported literatures.[27,28] Apple-green liquid of bismuth complex was obtained, which did not dissolve in ethanol or water.

Synthesis of ionic liquid ($C_{16}MIMBF_4$)

1-Hexadecyl-3-methylimidazolium-bromide ($C_{16}MIMBr$) was synthesized by a reaction of mixing 0.25 mol of 1-methylimidazole with 0.25 mol of 1-bromohexadecane at 90 °C for 24 h. The product was purified by recrystallization in tetrahydrofuran (THF). The resulting white crystals were collected by filtration and dried under vacuum at 60 °C. Then, a solution of $NaBF_4$ (8.50 g, 0.077 mol) in water (50 mL) was added slowly to a rapidly stirring solution of $C_{16}MIMBr$ (30 g, 0.077 mol) in water (250 mL). The waxy solids precipitated and collected by filtration. Then it was dissolved in dichloromethane (150 mL) and washed with 100 mL of water three times. The organic phase was collected and dried with anhydrous $MgSO_4$. After filtering, the organic solvent was removed in vacuum to yield the tetrafluoroborate salt ($C_{16}MIMBF_4$, 22.68 g, 74%). ^1H NMR was recorded at room temperature and *J* values were given in Hz. δ_H(400 MHz; $CDCl_3$; Me_4Si) 8.96 (1 H, s, CH), 7.27 (1 H, s, CH), 7.21 (1 H, s, CH), 4.16 (2 H, t, J_{AB} 7.4, CH_2), 3.96 (3 H, s, CH_3), 1.82–1.90 (2 H, m, CH_2), 1.20–1.32 (26 H, m, $C_{13}H_{26}$) and 0.85 (3 H, t, J_{AB} 6.4, CH_3).

Synthetic process of Bi_2S_3 nanocrystals

$C_{16}MIMBF_4$ (0.8 g) in a cuvette was heated to 165 °C with an oil bath to make it melted, then 0.085 g of $Bi[S_2P(OC_8H_{17})_2]_3$ was added. After shaking, the color of the solution turned to dark gray quickly, indicating the formation of Bi_2S_3. The reaction mixture was kept at 165 °C for different times. After the reaction finished, the resulting solution was cooled to room temperature naturally and the mixture became solid state. Afterwards, ethanol was added to make it dissolved. The Bi_2S_3 nanocrystals were collected by centrifugation and thoroughly washed with ethanol.

Electrochemical measurements

The electrochemical measurements were carried out following the reported method[29] at 25 °C. The electrode was fabricated by directly pressing the synthesized Bi_2S_3 powders to a sheet of nickel foam at 18 MPa. All of the experiments were carried out with a three-electrode system in 5 M KOH electrolyte under normal atmosphere, in which the Bi_2S_3 nanocrystals were used as the working electrode, $Ni(OH)_2$/NiOOH as the counter electrode, and Hg/HgO as the reference electrode. The Bi_2S_3 electrode was charged for 2 h at a current density of 50 mA g^{-1} and discharged at the same current density after a 60 s rest. The charge-discharge measurements were carried out using the Land battery system (CT2001A). Cyclic voltammograms measurements were performed on a CHI 660C electrochemical workstation.

Acknowledgements

This work was supported by the NFSC (Grant No. 20803087) and the Major State Basic Research Development Program of China (973 Program) (Grant No. 2007CB607606).

Notes and references

1 S. A. Keneman, *Appl. Phys. Lett.*, 1971, **19**, 205.
2 W. Tokuda, T. Katoh and A. Yasumori, *J. Appl. Phys.*, 1974, **45**, 5098.
3 R. Frerichs, *J. Opt. Soc. Am.*, 1953, **43**, 1153.
4 J. Black, E. M. Conwell, L. Seigle and C. W. Spencer, *J. Phys. Chem. Solids*, 1957, **2**, 240.

5 R. Suarez, P. K. Nair and P. V. Kamat, *Langmuir*, 1998, **14**, 3236.
6 R. R. Ahire, N. G. Deshpande, Y. G. Gudage, A. A. Sagade, S. D. Chavhan, D. M. Phase and R. Sharma, *Sens. Actuators, A*, 2007, **140**, 207.
7 B. Zhang, X. Ye, W. Hou, Y. Zhao and Y. Xie, *J. Phys. Chem. B*, 2006, **110**, 8978.
8 X. Yu, C. Cao and H. Zhu, *Solid State Commun*., 2005, **134**, 239.
9 (*a*) Z. Liu, S. Peng, Q. Xie, Z. Hu, Y. Yang, S. Zhang and Y. Qian, *Adv. Mater*., 2003, **15**, 936; (*b*) J. Ota and S. K. Srivastava, *J. Phys. Chem. C*, 2007, **111**, 12260; (*c*) Q. Han, J. Chen, X. Yang, L. Lu and X. Wang, *J. Phys. Chem. C*, 2007, **111**, 14072.
10 M. B. Sigman, Jr. and B. A. Korgel, *Chem. Mater*., 2005, **17**, 1655.
11 Q. Lu, F. Gao and S. Komarneni, *J. Am. Chem. Soc*., 2004, **126**, 54.
12 L. Tian, H. Y. Tan and J. J. Vittal, *Cryst. Growth Des*., 2008, **8**, 734.
13 J. Jiang, S. H. Yu, W. T. Yao, H. Ge and G. Z. Zhang, *Chem. Mater*., 2005, **17**, 6094.
14 (*a*) L. Manna, D. J. Milliron, A. Meisel, E. C. Scher and A. P. Alivisatos, *Nat. Mater*., 2003, **2**, 382; (*b*) A. J. Mieszawska, R. Jalilian, G. U. Sumanasekera and F. P. Zamborini, *Small*, 2007, **3**, 722.
15 (*a*) J. Dupont, R. F. de Souza and P. A. Z. Suarez, *Chem. Rev*., 2002, **102**, 3667; (*b*) P. Wasserscheid and W. Keim, *Angew. Chem., Int. Ed*., 2000, **39**, 3772; (*c*) A. E. Visser, R. P. Swatloski, W. M. Reichert, R. Mayton, S. Sheff, A. Wierzbicki, J. H. Davis, Jr. and R. D. Rogers, *Chem. Commun*., 2001, 135; (*d*) J. G. Huddleston, H. D. Willauer, R. P. Swatloski, A. E. Visser and R. D. Rogers, *Chem. Commun*., 1998, 1765; (*e*) M. C. Buzzeo, R. G. Evans and R. G. Compton, *ChemPhysChem*, 2004, **5**, 1106.
16 M. Antonietti, D. Kuang, B. Smarsly and Y. Zhou, *Angew. Chem., Int. Ed*., 2004, **43**, 4988.
17 A. Elaiwi, P. B. Hitchcock, K. R. Seddon, N. Srinivasan, Y. M. Tan, T. Welton and J. A. Zora, *J. Chem. Soc., Dalton Trans*., 1995, 3467.
18 T. Nakashima and N. Kimizuka, *J. Am. Chem. Soc*., 2003, **125**, 6386.
19 H. Itoh, K. Naka and Y. Chujo, *J. Am. Chem. Soc*., 2004, **126**, 3026.
20 B. G. Trewyn, C. M. Whitman and V. S.-Y. Lin, *Nano Lett*., 2004, **4**, 2139.
21 Y. Wang and H. Yang, *J. Am. Chem. Soc*., 2005, **127**, 5316.
22 X. D. Mu, J. Q. Meng, Z. C. Li and Y. Kou, *J. Am. Chem. Soc*., 2005, **127**, 9694.
23 R. Malakooti, L. Cademartiri, Y. Akcakir, S. Petrov, A. Migliori and G. A. Ozin, *Adv. Mater*., 2006, **18**, 2189.
24 Z. Liu, D. Xu, J. Liang, W. Lin, W. Yu and Y. Qian, *J. Solid State Chem*., 2005, **178**, 950.
25 L. Li, N. Sun, Y. Huang, Y. Qin, N. Zhao, J. Gao, M. Li, H. Zhou and L. Qi, *Adv. Funct. Mater*., 2008, **18**, 1194.
26 X. Chen, X. P. Gao, H. Zhang, Z. Zhou, W. K. Hu, G. L. Pan, H. Y. Zhu, T. Y. Yan and D. Y. Song, *J. Phys. Chem. B*, 2005, **109**, 11525.
27 W. Lou, M. Chen, X. Wang and W. Liu, *Chem. Mater*., 2007, **19**, 872.
28 S. L. Lawton, C. J. Fuhrmeister, R. G. Haas, C. S. Jarman, Jr. and F. G. Lohmeyer, *Inorg. Chem*., 1974, **13**, 135.
29 G. P. Dai, C. Liu, M. Liu, M. Z. Wang and H. M. Cheng, *Nano Lett*., 2002, **2**, 503.